Vibration control of platform structures with magnetorheological elastomer isolators based on an improved SAVS law

Vibration control of platform structures with magnetorheological elastomer isolators based on an improved SAVS law

Zhao-Dong Xu[1], Si Suo[2] and Yong Lu[3]

[1]Key Laboratory of C&PC Structures of the Ministry of Education, Southeast Univ., Si-Pai Lou 2#, Nanjing 210096, China, E-mail: xuzhdgyq@seu.edu.cn

[2]Key Laboratory of C&PC Structures of the Ministry of Education, Southeast Univ., Si-Pai Lou 2#, Nanjing 210096, China, E-mail: xjtu_ss@163.com

[3]Institute for Infrastructure and Environment, School of Engineering, The University of Edinburgh, Edinburgh EH9 3JL, UK, Email: yong.lu@ed.ac.uk

Abstract

This paper presents a study on the vibration control of platform structures with magnetorheological elastomer (MRE) isolators. Firstly, a novel MRE isolator design is put forward based on the mechanical properties of MREs, and subsequently a single-degree-of-freedom (SDOF) dynamic model and a multiple-degree-of-freedom (MDOF) dynamic model for platform systems incorporating such isolators are developed. In order to overcome the shortcomings of the conventional on-off control law, an improved semi-active variable stiffness (SAVS) control law is proposed. The proposed SAVS scheme makes full use of the continuously variable stiffness of MREs, and it takes into account the influence of the sampling interval such that the field-dependent restoring force is made to do negative work during the whole sampling interval as far as possible. The results of numerical simulations demonstrate that the improved SAVS control law can achieve better vibration-control effectiveness than the on-off control law. The comparative results are discussed through examining the mechanisms of these two control laws in light of the power spectral density (PSD) and the energy input. For an MDOF platform a simplified approach is proposed to combine the local response signals with an

equivalent SDOF representation to generate the control parameters for individual isolators, and the effectiveness of such a scheme is also verified through numerical simulation.

Keywords: semi-active vibration control, platform, MRE isolators, SAVS, control law

1. Introduction

A structural platform is often used to accommodate sensitive payloads such as laser systems. Such a platform must be maintained in a virtually vibration-free status to ensure the precision and stability of the payloads when subjected to environmental disturbance of a wide frequency range [1]. Thus, the vibration control of such platforms has recently received significant attention.

A variety of vibration isolation techniques may be adopted, including passive isolation, active isolation and semi-active isolation. Passive isolators such as rubber layers and spring supports can be effective in a limited frequency band, but they may perform unsatisfactorily under broad-band environmental excitations due to their pre-defined mechanical parameters. Therefore, increasing attention has been drawn to the active and semi-active isolation. In the active isolation arena, there are a range of devices developed for the vibration control of platform structures. Zhang et al. [2] developed an active vibration isolation system for a micro-manufacturing platform using strongly magnetostrictive actuators. Nakamura et al. [3-4] designed a micro-vibration control system with hybrid actuators comprising air actuators and giant magnetostrictive actuators, and demonstrated through the control experiments that hybrid actuators performed more effectively than air actuators alone under various disturbances. Kim and Cho et al. [5] proposed a conceptual design of a novel 3-DOF micro-stage for active micro-vibration control using a piezoelectric transducer and a flexural hinge mechanism as an actuation unit, which made the whole structure compact, light and simple. However, active isolation has limits due to problems like actuator saturation, high cost and especially high energy consumption, and these factors become more restrictive for a platform with large

payloads.

With the development of semi-active control techniques, more and more semi-active actuators are applied in vibration control with magnetorheological damper (MRD) taking a lead due to its variable damping forces as well as less power consumption compared with active-control devices. In broader applications, MRD has been applied in protecting civil infrastructure systems against severe earthquake and wind loading [6], in semi-active seat suspension systems [7] and in payload launch vibration isolation of a spacecraft [8]. However, there are some inherent problems with the use of MR fluids such as iron particle settlement and the difficulty of sealing the fluids.

Compared with MR fluids, magnetorheological elastomers (MREs) possess several advantages. Firstly, MRE is a sort of magnetorheological material whose magnetic particles are aligned and dispersed in a solid polymer matrix like rubber, and therefore MRE is more stable and easier to be manufactured into various shapes to fit to different devices. Furthermore, MRE has a variable modulus, which is another essential mechanical property and can be controlled by external magnetic fields and revert to its original status immediately when the magnetic field is removed. This property enables MRE to perform more effectively than MRD in controlling a low-frequency and high-amplitude vibration [9] by achieving both a desired restoring force (depending on the vibration amplitude) and a high damping force (depending on the velocity, and hence the vibration frequency, and damping change due to magnetic field is lower than stiffness change, which can be neglected).

A variety of applications with MREs have been proposed and developed in recent years. Ginder et al. [10] designed and built a proof-of-concept MRE bushing.

Li et al. [11] propose a conceptual design of a seat suspension system using MRE isolator and conducted a range of tests, the results of which showed that the developed MRE isolator is able to reduce vibration more than the passive isolation system. Liao et al. [12] presented a type of active-adaptive tuned vibration absorber based on MRE and investigated its mechanical properties experimentally, indicating the significant potential of its application in vibration control. Behrooz et al. [13] proposed a new MRE isolator (VSDI) and tested the effectiveness of using multiple such isolators in the control of seismic response on a three-story scaled building model, and the experimental results showed that the VSDIs significantly reduced the acceleration and relative displacement of the building floors. The above studies demonstrate that by adjusting the stiffness of the MRE isolators in real-time, the isolation system can keep the controlled object away from resonance and thus further suppress the vibration.

On the other hand, the control law is another important factor on the vibration-control effectiveness. The on-off control law is adopted widely in semi-active control systems involving variable stiffness (SAVS) due to its simplicity and general effectiveness [14], but it is not suitable for the MRE isolators because this control law only utilizes two states of the isolators, namely the maximum stiffness and the minimum stiffness, while MRE isolators can exhibit continuous variable stiffness. In search for better control schemes for MRE isolators, Yang et al. [15] presented a control method based on the theory of sliding mode control (SMC), and their simulation results indicated that this method was robust in terms of displacement and velocity control, but performed poorly on controlling the acceleration of the structure. Besides, the drawback of SMC in terms of chattering

also adversely influenced the vibration isolation effectiveness. Du et al. [9] designed an H_∞ controller based on an integrated seat suspension model, and their results of simulations suggested that this method achieved more effective performance than the on-off control law. However, the control law based on the H_∞ theory has a complex formation and a minimization problem must be solved, which makes it difficult to be applied in practice.

In this study, a novel MRE isolator design is put forward taking advantage of the key mechanical properties of MREs, particularly the field-dependent stiffness as well as damping. A dynamic model of a platform involving such an isolator is formulated using a single-degree-of-freedom (SDOF) representation first, and the model is then extended to a multiple-degree-of-freedom (MDOF) system. To achieve a desired control effect, an improved SAVS algorithm is proposed, taking into account the effect of sampling intervals, so as to overcome the drawbacks of the conventional on-off control law. The proposed algorithm has clear physical meanings and has also relatively simple formation. A range of numerical simulations on an SDOF system and an MDOF system, respectively, are conducted. The results suggest that the improved SAVS control law performs more effectively than the on-off control law on vibration control of a platform structure under wide-band environmental excitations. An analysis of the results also explains the mechanism of the improved effectiveness from the viewpoints of the PSD and the energy input.

2. Concept design of MRE isolator

2.1 Mechanical properties of MREs

In this study, the MRE under consideration is a type of anisotropic materials. The

experimental characterization of this material was carried out in a previous study by the authors [16]. The main physical and mechanical properties are briefly summarized in what follows.

The MRE is a composite of polymer matrix and ferromagnetic particles. In this study, bromobutyl rubber (BIIR) is adopted as the matrix material because of its high damping capacity, and it is filled with 3.3-μm carbonyl iron powder. BIIR was mixed with carbonyl iron particles (454.8phr) and some additives (reinforcing agent 45phr, plasticizing agent 15phr, vulcanizing agent 13.9phr, catalytic agent 21phr) in a two-roll mill (XK-400). Then, the mixture was filled into a mold to pre-form at 135°C for 15 minutes under a constant magnetic flux density of 100mT which was generated by two high temperature-resistant permanent magnets. After being vulcanized at 165°C for 30min in a plate vulcanization machine (TH-6009), the MRE sample was finished.

In order to investigate the mechanical properties of MREs, dynamic tests are conducted using an MTS hydraulic actuator and the constant magnetic field ranging from 0 to 300mT can be applied through a magnetic field generating device, as shown in Figure 1. By applying a certain sinusoidal excitation (1mm, 5Hz in this study) under various magnetic flux intensity (0, 100, 200 and 300mT), the force-displacement loops were obtained, as shown in Figure 2. Based on the viscoelastic theory, when the MRE sample was tested under a harmonic input $u(t)=u_0\sin(\omega\cdot t)$, the response force can be expressed as [16]

$$F(t)=u_0\cdot\frac{m_v\cdot A_s}{t_s}\cdot\sqrt{G_1^{\,2}+G_2^{\,2}}\cdot\sin(\omega\cdot t+\phi) \tag{1}$$

where $F(t)$ is the response force, m_v is the numbers of the shear layer of MRE

specimens. A_s and t_s are the area and the thickness of the shear layer, respectively. ϕ is the phase angle difference between the displacement excitation and the response force, G_1 and G_2 are the storage modulus and the loss modulus of the MRE material, respectively.

The loss factor η that indicates the energy dissipation capacity of MRE materials can be written as $\eta = \frac{G_2}{G_1} = \tan\phi$. The parameters G_1 and η are determined by analyzing the data of force-displacement loops and they are shown in Figure 3, in which with the magnetic field ranging from 0 to 300mT, the shear storage modulus of the MRE sample increases from 1.20MPa to 1.50MPa by 25.0% and the loss factor is around 0.6. According to Figure 3, it is reasonable to predict that the shear storage modulus will rise under a more intense magnetic field. So, it is concluded that the MRE sample used in this study possesses remarkable changeable stiffness and good damping capacity.

2.2 Design of MRE isolator

In order to satisfy the need of platform vertical isolation, a concept design of the MRE isolators is made as shown in Figure 4. This isolator is mainly composed of the core, coils, MRE layers and housing. The isolator has two key features, namely a controllable stiffness and damping. The payload from the platform is transferred through the two MRE layers to the housing and then to the base, thus the stiffness of the whole support depends on the shear modulus of MRE layers. Furthermore, the core and housing are made from magnetism materials and so the coils, core and housing form a closed magnetic circuit, which can generate changeable magnetic fields for MRE layers. Based on the above design, the stiffness of the isolator can be

adjusted to satisfy the particular need in real time by controlling the current intensity of coils. On the other hand, the MRE layers also supply the effective damping to the whole system, which can reduce the vibration and dissipate the input energy.

3. Theoretical models for platform structure

3.1 Single-degree-of-freedom system

For some small-size platforms, such as the micro-manufacturing platform, the single support set in the middle of the platform can guarantee the bearing capacity and stability of the whole structure. This kind of platform can be simplified as an SDOF system which has only vertical degree of freedom, as shown in Figure 5.The equilibrium equation of motion can be expressed as

$$m \cdot \ddot{z}(t) + c \cdot \dot{z}(t) + (k_0 + k_m) \cdot z(t) = f(t) \tag{2}$$

where m is the total mass of the platform; c is the damping factor; k_0 is the zero-field stiffness of the MRE isolator and k_m is the field-dependent stiffness; $f(t)$ is the environmental excitation; $z(t)$, $\dot{z}(t)$ and $\ddot{z}(t)$ are the vertical displacement, velocity and acceleration of the platform, respectively.

3.2 Multiple-degree-of-freedom system

For most big-size rectangular platforms with large loads, there are usually four supports located on the corner points for the sake of stability and safety. Therefore, besides the vertical degree of freedom, two lateral-flip degrees of freedom (X-rotation and Y-rotation) should be taken into account for this kind of platform structures and it can be simplified as an MDOF system, as shown in Figure 6, where $2a$ and $2b$ are the edge lengths of the platform; m_z, I_x and I_y are the total

mass, X-rotation moment of inertia and Y-rotation moment of inertia of the platform, respectively; u, θ_x and θ_y are the vertical displacement, X-rotation angular displacement and Y-rotation angular displacement of the platform, respectively. For the four supports, u_A, u_B, u_C and u_D are vertical displacements; k_{A0}, k_{B0}, k_{C0} and k_{D0} are zero-field stiffness; k_{Am}, k_{Bm}, k_{Cm} and k_{Dm} are field-dependent stiffness; c_A, c_B, c_C and c_D are damping factors, respectively.

The stiffness of the platform is usually much larger than that of the supports; therefore it is reasonable to assume that the platform undergoes only a rigid body motion. On this basis, the governing equations of motion can be established according to Hamilton's principle and this is briefly described as follows. Firstly, the kinetic energy T, potential energy V and work done by non-conservative forces W_{nc} of the MDOF system in Figure 6 are expressed as

$$T = \frac{1}{2} m_z \cdot \dot{u}_z^{\,2} + \frac{1}{2} I_x \cdot \dot{\theta}_x^{\,2} + \frac{1}{2} I_y \cdot \dot{\theta}_y^{\,2} \tag{3}$$

$$V = \frac{1}{2} \sum_{i=A..D} k_i \cdot u_i^{\,2} \tag{4}$$

$$W_{nc} = -\sum_{i=A..D} c_i \cdot \dot{u}_i \cdot u_i \tag{5}$$

Substitute (3), (4) and (5) into the Hamilton's formation

$$\int_{t_1}^{t_2} \delta(T - V) \cdot dt + \int_{t_1}^{t_2} \delta W_{nc} \cdot dt = 0 \tag{6}$$

and simplify it as

$$\mathbf{M} \cdot \ddot{\mathbf{X}} + \mathbf{C} \cdot \dot{\mathbf{X}} + \mathbf{K} \cdot \mathbf{X} = \mathbf{D_s} \cdot \mathbf{F} \tag{7}$$

where,

$$\mathbf{X}=\begin{bmatrix} u_z \\ \theta_x \\ \theta_y \end{bmatrix},\quad \mathbf{F}=\begin{bmatrix} F_z \\ M_x \\ M_y \end{bmatrix},\quad \mathbf{M}=\begin{bmatrix} m_z & & \\ & I_x & \\ & & I_y \end{bmatrix}$$

$$\mathbf{K}=\begin{bmatrix} \sum_{i=A..D} k_i & b\cdot\left(-k_A-k_B+k_C+k_D\right) & a\cdot\left(-k_A+k_B+k_C-k_D\right) \\ b\cdot\left(-k_A-k_B+k_C+k_D\right) & b^2\cdot\sum_{i=A..D} k_i & a\cdot b\cdot\left(k_A-k_B+k_C-k_D\right) \\ a\cdot\left(-k_A+k_B+k_C-k_D\right) & a\cdot b\cdot\left(k_A-k_B+k_C-k_D\right) & a^2\cdot\sum_{i=A..D} k_i \end{bmatrix}$$

$$\mathbf{C}=\begin{bmatrix} \sum_{i=A..D} \mathrm{c}_i & b\cdot\left(-c_A-c_B+c_C+c_D\right) & a\cdot\left(-c_A+c_B+c_C-c_D\right) \\ b\cdot\left(-c_A-c_B+c_C+c_D\right) & b^2\cdot\sum_{i=A..D} c_i & a\cdot b\cdot\left(c_A-c_B+c_C-c_D\right) \\ a\cdot\left(-c_A+c_B+c_C-c_D\right) & a\cdot b\cdot\left(c_A-c_B+c_C-c_D\right) & a^2\cdot\sum_{i=A..D} c_i \end{bmatrix}$$

$$\mathbf{D_s}=\begin{bmatrix} 1 & 1 & 1 & 1 \\ -b & -b & b & b \\ -a & a & a & -a \end{bmatrix}$$

4. Improved SAVS algorithm

4.1 Conventional on-off algorithm

Since the MRE isolator has a semi-active character, the dynamic property of the whole structure can be adjusted to avoid resonance. On the other hand, the vibration-reduction function of the MRE isolator can be activated or deactivated based on the vibration energy input. Taking an SDOF system for example, when the direction of displacement u is the same as that of velocity $\dot{u}$, that is, $u\cdot\dot{u}>0$, the work by the field-dependent restoring force F_{sm} ($F_{sm}=-k_m\cdot u$) equals $k_m\cdot u\cdot\dot{u}\cdot\Delta t<0$, which means the additional stiffness leads to a negative work and dissipate the vibration energy input; conversely, when u and $\dot{u}$ have the opposite directions, any additional stiffness can result in a positive work and consequently

make the system absorb the excitation energy and thus intensifies the vibration.

Based on the above analysis, a conventional on-off control law for an MRE isolator as proposed in [13] can be established as

$$k_m = \begin{cases} k_{m,\max} & u \cdot \dot{u} > 0 \\ 0 & u \cdot \dot{u} \le 0 \end{cases} \tag{8}$$

where $k_{m,\max}$ is the upper limit of field-dependent stiffness of the MRE isolator.

4.2 Improved SAVS algorithm

Although the conventional on-off control can reduce the vibration, especially the low-frequency response of the system [13], there are some drawbacks in this control law. Firstly, the field-dependent stiffness of the MRE isolator k_m is given only two choices, namely the maximum and minimum value, but in fact MRE has continuously variable stiffness and this is not fully exploited in the on-off control. Secondly, because of the existence of the sampling interval Δt, the collected signals of u and $\dot{u}$ are discrete, and so there is no guarantee that $u \cdot \dot{u} > 0$ during the whole sampling interval if $k_{m,\max}$ is the only choice of k_m. An example of such a scenario is when the response approaches a peak displacement, as shown in Figure 7. In such a case it could happen that when $t = t_1$ (a sampling time point), $u \cdot \dot{u} > 0$ but $\dot{u}$ is very small, and when $t = t_{1a}$ ($t_1 < t_{1a} < t_2$), $\dot{u} = 0$ and when $t = t_2$ (the next sampling time point), $u \cdot \dot{u} < 0$. By the on-off law k_m will adopt the maximum stiffness $k_{m,\max}$ for the whole time interval from t_1 to t_2. But actually during the time from t_{1a} to t_2, the field-dependent restoring force F_{sm} is doing positive work that can intensify the vibration. Obviously this drawback of the on-off control will tend to become more pronounced when high-frequency response is involved.

Based on the above analysis, a semi-active variable stiffness (SAVS) algorithm is proposed to overcome the shortcomings of the conventional on-off control law and improve the control efficiency. The optimum stiffness of the MRE isolator can be defined as such that the velocity $\dot{u}$ of the controlled object becomes zero at the end of the sampling interval Δt, i.e. $\dot{u}=0$ when $t=t_2$, which means the field-dependent restoring force F_{sm} is doing negative work during the whole sampling interval Δt. To this end, an effective algorithm is needed to predict such stiffness according to the current state ($t=t_1$) of the controlled object and environmental excitation. In this study, the Newmark-β method [17] ($\gamma=\frac{1}{2}$, $\beta=\frac{1}{6}$) is adopted as a predictor of field-dependent stiffness k_m. For an SDOF system,

$$m\cdot\ddot{u}(t)+c\cdot\dot{u}(t)+(k_0+k_m)\cdot u(t)=f(t) \tag{9}$$

The formation of the Newmark-β method can be expressed as

$$u_{t+\Delta t}=\frac{\tilde{f}}{\tilde{k}} \tag{10}$$

$$\dot{u}_{t+\Delta t}=\frac{3}{\Delta t}\cdot(u_{t+\Delta t}-u_t)-2\dot{u}_t-\frac{\Delta t}{2}\ddot{u}_t \tag{11}$$

where the effective stiffness $\tilde{k}=k_0+k_m+\frac{3c}{\Delta t}+\frac{6m}{\Delta t^2}$ and the effective load $\tilde{f}=f(t)+m\cdot\left(\frac{6u_t}{\Delta t^2}+\frac{6\dot{u}_t}{\Delta t}+2\ddot{u}_t\right)+c\cdot\left(\frac{3u_t}{\Delta t}+2\dot{u}+\frac{\Delta t\cdot\ddot{u}_t}{2}\right)$. Considering the condition that $\dot{u}_{t+\Delta t}=0$, the field-dependent stiffness k_m is obtained by solving the above equations,

$$k_m = \frac{f(t) + m \cdot \left(6u_t / \Delta t^2 + 6\dot{u}_t / \Delta t + 2\ddot{u}_t\right) + c \cdot (3u_t / \Delta t + 2\dot{u}_t + \ddot{u}_t \cdot \Delta t / 2)}{u_t + \left(2\dot{u}_t + \ddot{u}_t \cdot \Delta t / 2\right) \cdot \Delta t / 3} - 3c / \Delta t + 6m / \Delta t^2 - k_0 \quad (12)$$

In addition, k_m calculated by (12) must be subject to the constraint of the maximum $k_{m,\max}$ due to the limit of the magnetorheological effect of MREs, and it should also be no less than zero.

On the above basis, the improved SAVS control law can be described as follows,

Step 1:

Calculate the optimal $\tilde{k}_m$ according to (12),

$$\tilde{k}_m = \frac{f(t) + m \cdot \left(6u_t / \Delta t^2 + 6\dot{u}_t / \Delta t + 2\ddot{u}_t\right) + c \cdot (3u_t / \Delta t + 2\dot{u}_t + \ddot{u}_t \cdot \Delta t / 2)}{u_t + \left(2\dot{u}_t + \ddot{u}_t \cdot \Delta t / 2\right) \cdot \Delta t / 3} - 3c / \Delta t + 6m / \Delta t^2 - k_0 \quad (13)$$

Step 2: determine the actual k_m,

$$k_m = \begin{cases} k_{m,\max} & \tilde{k}_m \geq k_{m,\max} \ and \ u \cdot \dot{u} > 0 \\ \tilde{k}_m & 0 < \tilde{k}_m < k_{m,\max} \ and \ u \cdot \dot{u} > 0 \\ 0 & u \cdot \dot{u} \leq 0 \ or \ \tilde{k}_m < 0 \end{cases} \quad (14)$$

Compared with the conventional on-off control law, the proposed SAVS requires the collection of the acceleration $\ddot{u}$ of the controlled object and the external excitation $f(t)$ additionally, but it has an enhanced basis for more robust control performance, as will be demonstrated in the numerical simulations in the next section.

5. Numerical simulations

In this section, numerical simulations for an SDOF system and an MDOF system are conducted in MATLAB to verify the effectiveness of the improved SAVS algorithm by comparing with the conventional on-off control law.

In these simulations, we assume that the maximum magnetorheological effect of MREs used in this study can reach 200%, i.e. $k_{m,\max} = k_0$, and its damping capacity does not vary significantly with the magnetic field, so the damping factor c can be regarded as a constant. In addition, the environmental excitations (including vertical acceleration $\ddot{z}_g$ and two angular accelerations $\ddot{\theta}_{xg}$ and $\ddot{\theta}_{yg}$) are assumed to be broad-band and they are generated according to a power spectral density curve as shown in Figure 8.

For the sake of convenience, an indicator η, defined in Equation (15), is introduced to compare the vibration control effectiveness among different algorithms.

$$\eta = \frac{|x_{un}|_{\max} - |x|_{\max}}{|x_{un}|_{\max}} \times 100\% \tag{15}$$

where x denotes the responses of the system with the control in place (by the on-off law or the improved SAVS law), including displacement d, velocity v and acceleration a; x_{un} denotes the uncontrolled responses, namely the responses of the passive system.

5.1 Single-degree-of-freedom system

An SDOF platform is considered first. The parameters of the SDOF platform are listed as follows: total mass (including the components of the payload and the platform structure) $m = 150\,\text{kg}$, zero-field stiffness $k_0 = 8\times10^5\,\text{N/m}$, damping factor $c = 9\times10^2\,\text{N}\cdot\text{s/m}$.

For a sampling frequency $f_s = 100\,\text{Hz}$ ($\Delta t = 0.01\,\text{s}$), the responses of the SDOF system without any control, with the on-off control, and with the improved SAVS

control, respectively, are computed and the results are compared in Figure 9.

As can be seen from Figure 9, for the passive system there is a marked resonance periods at around 1.5s when the responses of the system without any control are amplified significantly, even larger than the excitation, suggesting that passive control alone cannot satisfy the requirement of vibration mitigation. However, such resonance effects are virtually eliminated in the responses of the controlled system adopting either the on-off law or the improved SAVS law. This indicates that both control laws are effective in controlling the resonance responses. Further inspection of the results between the on-off law and the improved SAVS law reveals that the response of the system controlled by the improved SAVS law is smaller than that by the on-off law in the majority of the time frame, and this is particularly true for the velocity and displacement time histories.

The above observation is also supported by the indicator η, as shown in Table 1. In fact, the results in Table 1 suggest that the improved SAVS law performs better than the on-off law in all terms of the system responses. Most notably, the velocity of the platform is reduced by 34% and maintained at less than 0.05m/s level by using the improved SAVS law. Both of these two algorithms exhibit the least controlling effect in terms of the platform acceleration, with the η value being 3% for on-off control and 14% for improved SAVS control.

In order to study the vibration-reducing mechanism of these two control laws, a further comparison is conducted firstly on PSD of the acceleration response, as shown in Figure 10. The natural frequency of the SDOF system is around 11.72Hz obtained from the PSD curve of the passive system. Compared with the passive system, the resonant frequency of a controlled system with either SAVS law will

shift to a bigger value (14.65Hz for on-off law and 12.70Hz for improved SAVS law) because the MRE isolator can provide extra stiffness. Furthermore, the PSD peaks of both controlled systems are lowered and the both curves appear plumper than that of the passive system as a whole, suggesting that a controlled system possesses greater damping effect, and obviously the system with the improved SAVS law is superior to that with the on-off law on such respect.

Another comparison is conducted on the energy input and the changing stiffness. Generally speaking, the energy of a dynamic system consists of elastic potential energy E_k and kinetic energy E_v, and the damping of the system dissipates a part of the energy absorbed from the environmental excitation, namely E_d.The sum of these three parts equals the total input energy E_{in}, i.e., $E_{in} = E_k + E_v + E_d$.

The time histories of total input energy of the system without and with the two different control schemes are shown in Figure 11. As can be seen, first of all, the overall trend of all of the three curves is upward since the damping is dissipating energy all the time while there are large and small fluctuations due to the frequent variation of the elastic potential energy E_k and the kinetic energy E_v.For the passive system, there is a period (circled in Figure 11) during which E_{in} of the system increases dramatically and this period correspond to the aforementioned resonance period, indicating that the resonance can lead to a surge of E_{in}, as expected. In comparison, the overall increase of E_{in} for a controlled system is markedly smoother and steadier, although there are still some but less significant jumps.

The change of k_m determined by these two control laws, over a time window

of 3~4s, is compared in Figure 12. From the zoom-in energy input E_{in} curves shown in Figure 12(a), we can see significant differences between these two curves at the circled periods, when E_{in} of the system using the on-off law surges remarkably while that using the improved SAVS law exhibit only moderate jumps. Examining Figure 12(b) it can seen that a more desirable stiffness k_m is obtained through the improved SAVS law, which helps the whole system avoid the resonance and thus control the vibration more effectively. Based on the above comparisons, it can be concluded that, by exploiting the variable stiffness property of MREs and enabling the adjustment of the stiffness on a continuous basis, the improved SAVS law achieves better performance than the on-off law on vibration controlling of a platform.

5.2 Multiple-degree-of-freedom system

For a platform supported via multiple supports and isolators, such as the case shown in Figure 6, an optimal control of the vibration will require a comprehensive scheme taking into account the combined effect among the isolators in a MDOF system. However, considering that at each isolator the vibration signal can be acquired individually and the global coupling effect due to the rigid platform is contained in the acquired signals at real time, it is possible to simplify the control by taking the real-time signal from the MDOF platform at individual isolators and generate the corresponding control parameters through a simplified SDOF associated with each individual isolator.

The idea is illustrated in Figure 13. For the generation of the field-dependent stiffness at each isolator while the vibration signal is taken locally from the MDOF platform, a “SDOF generator” is created for each support. Depending on the layout

of the supports, a proportion of the total system mass is allocated to the SDOF associated with each support. In the case shown in Figure 13 where the platform is supported equally at the four corners, each SDOF has a share of one-quarter of the total mass. Similarly to the SDOF system described in Section 4.2, the stiffness of each SDOF here consists of an invariable base stiffness k_0 and the field dependent stiffness k_m, and k_m will be determined using the chosen control law based on the locally acquired signals at each support. Thus, each isolator will respond with its individual field-dependent stiffness driven by the local "optimum" in generating negative work, and as such the isolators in combination are expected to achieve an effective control of the vibration of the MDOF platform.

As an example, an MDOF platform is numerically simulated. The parameters of the MDOF platform are as follows: side lengths $2a = 1.2\text{m}$ and $2b = 1\text{m}$; total mass $m_z = 250\,\text{kg}$, X-rotation moment of inertia $I_x = 21\,\text{kg}\cdot\text{m}^2$ and Y-rotation moment of inertia $I_y = 30\,\text{kg}\cdot\text{m}^2$; zero-field stiffness of each MRE isolator $k_0 = 2\times10^5\,\text{N/m}$, damping factor of each MRE isolator $c = 2.25\times10^2\,\text{N}\cdot\text{s/m}$. The sampling frequency is $f_s = 100\,\text{Hz}$.

The results of vibration accelerations including the platform center displacement $\ddot{u}_z$, and rotations $\ddot{\theta}_x$ and $\ddot{\theta}_y$ are illustrated in Figure 14. The vibration reduction indicator η from different control laws are listed in Table 2.

From Figure 14, it can be seen that both control laws achieve marked vibration-reduction effects on all three acceleration components, and this is particularly true at the resonance periods. As can be seen in Table 2, better controlling effects are achieved on the Z-displacement than on the rotations under both control

laws. This phenomenon may be attributed to the simplified use of individual SDOFs to generate control parameters, which essentially targets more directly on the vertical translation. Relatively speaking, the improved SAVS law achieves better performance than the on-off law. It should be noted that the two control laws performs less effectively on controlling the acceleration of the MDOF system than the displacement and the velocity. But between the two control laws the improved SAVS still performs better; more specifically the X-rotation and Y-rotation accelerations of the system tend to be out of control (η being -2% and -5%) under the on-off law, whereas with the improved SAVS law these rotational accelerations are virtually unaffected (η being 16% and -2%) while all other response parameters reduce significantly.

6. Conclusions

This paper presents a study on the vibration control of platform structures with MRE isolators. The design of the MRE isolators takes advantage of the dual mechanical properties of MREs, namely variable modulus (stiffness) as well as damping. An improved SAVS law is proposed with an aim to make full use of continuously variable stiffness of MREs so as to achieve enhanced control of the vibration. In particular, the improved SAVS scheme takes into account the influence of the sampling interval, and this provides a sound physical basis for the determination of desirable field-dependent stiffness at any time step.

Numerical simulations demonstrate that the proposed design scheme for the MRE isolators works well in general. The improved SAVS law exhibits notably better vibration-reduction effectiveness than the conventional on-off law, and this is particularly true in terms of suppressing resonant response. For an MDOF platform,

the simplified approach of combining the response signals acquired from the MDOF platform at individual supports (isolators) with a SDOF representation of the local dynamic response proves to be effective overall.

The results from the MDOF platform analysis also reveal that using the simplified approach the control on rotational displacements of the platform is less effective than on the vertical displacement. This is deemed to be attributable to the fact that rotational displacement is not directly targeted in the simplified SDOF scheme, and to achieve further improved control effect on a MDOF system the responses at different control points needs to be taking into account comprehensively and this should be considered in the future work.

Acknowledgments

Financial supports for this research are provided by the Outstanding Youth Natural Science Foundation of Jiangsu Province with Granted number BK20140025, Science and Technological Innovation Leading Young Talents Program of the Ministry of Science and Technology, Natural Science Foundation of Jiangsu Province with Granted number BK20141086, and the Fundamental Research Funds for the Central Universities. These supports are gratefully acknowledged.

References

[1] Geng Z J, Pan G G, Haynes L S, Wada B K and Garba J A, 1995, An intelligent control system for multiple degree-of-freedom vibration isolation, Journal of Intelligent Material Systems and Structures, 6, 787-800.

[2] Zhang C L, Mei D Q, and Chen Z C, 2002, Active vibration isolation of a micro-manufacturing platform based on the neural network, Journal of Materials Processing

Technology, 129, 634-639.
[3] Nakamura Y, Nakayama M, Yasuda M and Fujita T, 2006, Development of active six-degrees-of-freedom micro-vibration control system using hybrid actuators comprising air actuators and giant magnetostrictive actuators, Smart Materials and Structures, 15, 1133-1142.
[4] Nakamura Y, Nakayama M, Masuda K, Tanaka K, Yasuda M and Fujita T, 1999, Development of 6-DOF microvibration control system using giant magnetostrictive actuator Proceedings of SPIE, 3671, 229-240.
[5] Kim H S and Cho Y M, 2009, Design and modeling of a novel 3-DOF precision micro-stage, Mechatronics, 19, 598-608.
[6] Yang G, Spencer B F, Carlson J D and Sain M K, 2002, Large-scale MR fluid dampers: modeling and dynamic performance considerations, Engineering Structures, 24, 309-323.
[7] Choi S B, Nam M H and Lee B K, 2000, Vibration Control of a MR Seat Damper for Commercial Vehicles, Journal of intelligent material systems and structures, 11, 936-44.
[8] Jean P, Ohayon R and Bihan D, 2006, Semi-active control using magneto-rheological dampers for payload launch vibration isolation, Proc. SPIE, Smart Structures and Materials, 6169:61690H.
[9] Du H P, Li W H and Zhang N, 2011, Semi-active variable stiffness vibration control of vehicle seat suspension using an MR elastomer isolator, Smart Materials and Structures, 20, 105003-105012.
[10] Ginder J M, Nichols M E, Elie L D and Tardiff J L, 1999, Magnetorheological elastomers: properties and applications, SPIE, 3675, 131-138.
[11] Li W, Zhang X and Du H, 2012, Development and simulation evaluation of a magnetorheological elastomer isolator for seat vibration control, Journal of Intelligent Material Systems and Structures, 23, 1041-1048.
[12] Liao G J, Gong X L, Kang C J and Xuan S H, 2011, The design of an active-adaptive tuned vibration absorber based on magnetorheological elastomer and its vibration attenuation performance, Smart Materials and Structures, 20, 075015-075024.
[13] Behrooz M, Wang X and Gordaninejad F, 2014, Performance of a new magnetorheological elastomer isolation system, Smart Materials and Structures, 23, 045014-045021.
[14] Kobori T, Takahashi M, Nasu T, Niwa N and Ogasawara K, 1993, Seismic response controlled structure with active variable stiffness system, Earthquake Engineering and Structural Dynamics, 22, 925-941.
[15] Yang J N, Wu J C, Li Z, 1996, Control of seismic excited buildings using active variable stiffness systems, Engineering Structures, 18, 589-596.

[16] Zhu J, Xu Z and Guo Y, 2013, Experimental and modeling study on magnetorheological elastomers with different matrices, Journal of Materials in Civil Engineering, 25, 1762-1771.

[17] Clough R W, Penzien J, 1993, Dynamics of Structures McGraw-Hill, New York.

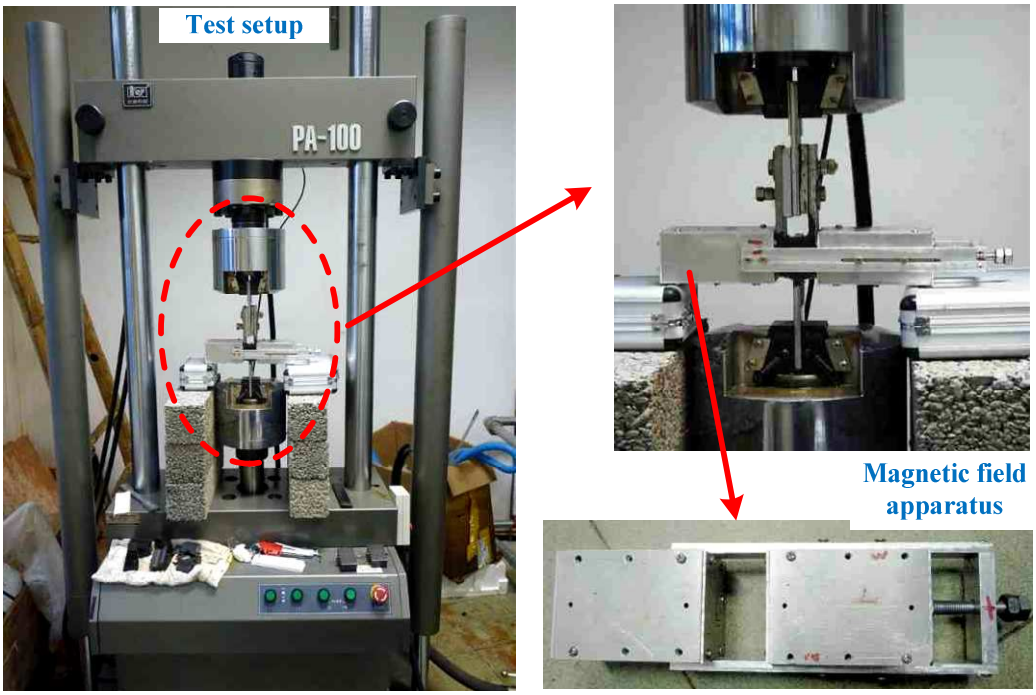

Figure 1 Experimental devices

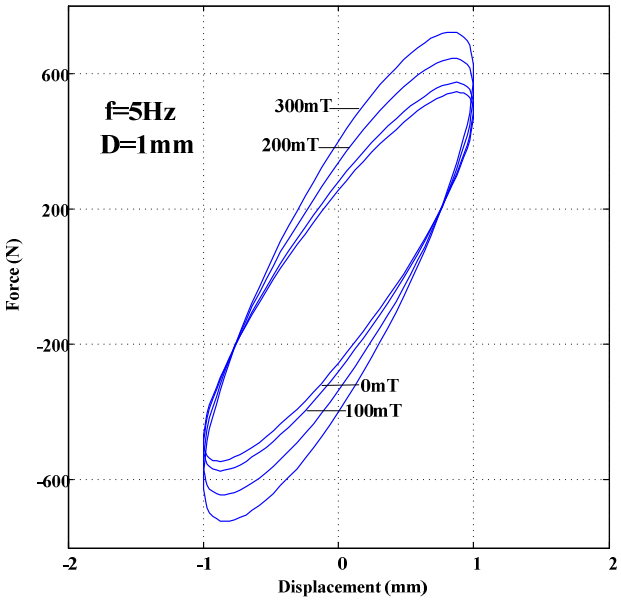

Figure 2 Force-displacement curves of MRE samples for different magnetic fields

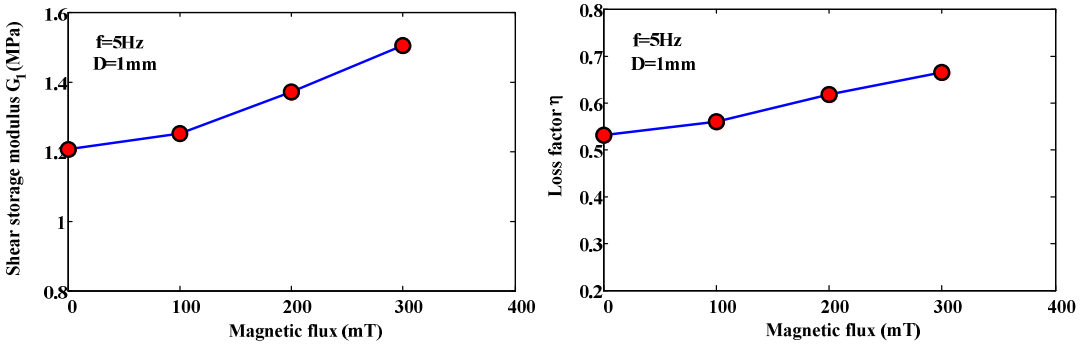

Figure 3 Shear storage modulus G1 and loss factor η for different magnetic fields

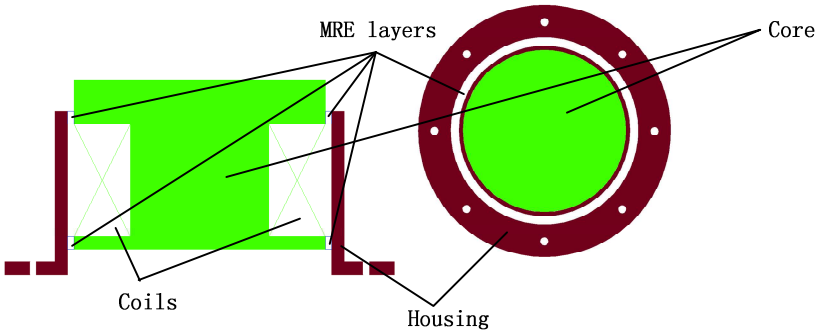

Figure 4 Concept design of the MRE isolator

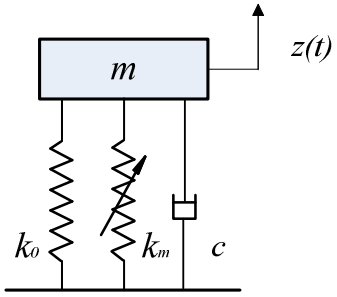

Figure 5 SDOF model for a controlled system with MRE isolator

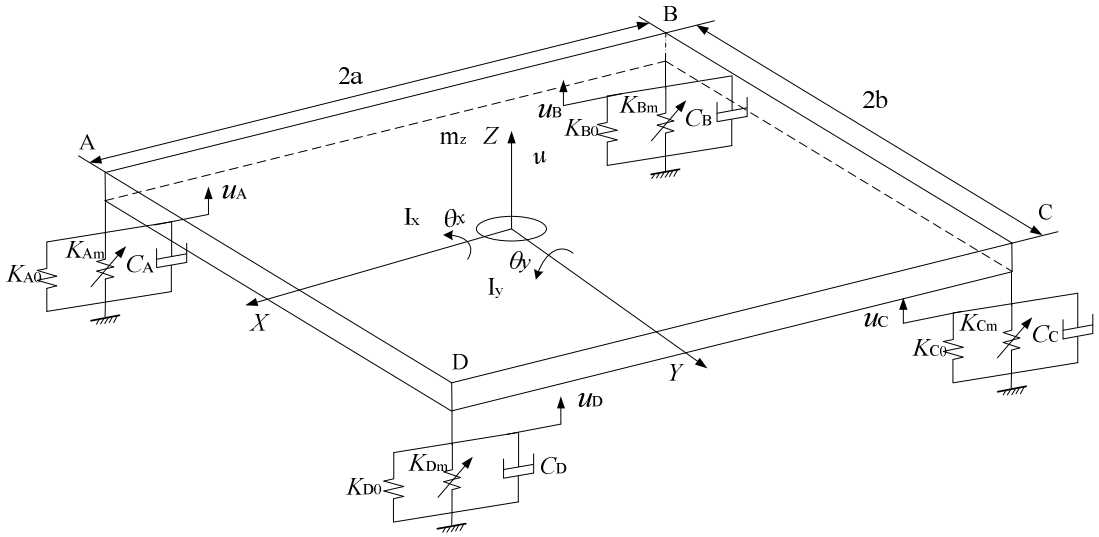

Figure 6 MDOF model for a platform with multiple MRE isolators

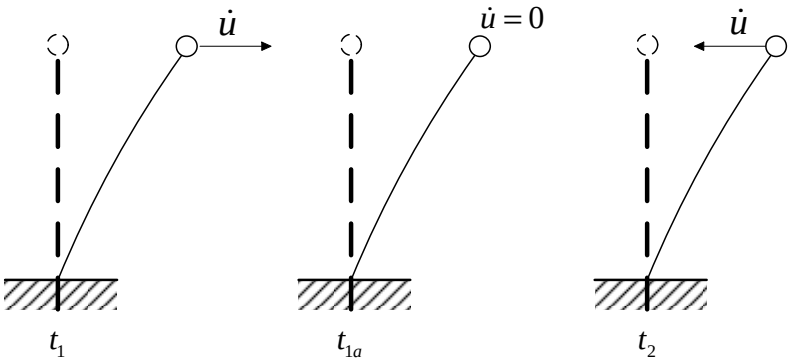

Figure 7 Illustration of possible states of a controlled object during a sampling interval

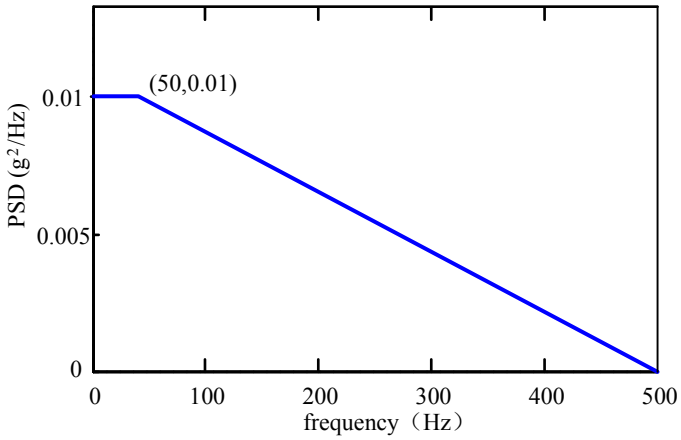

Figure 8 Power spectral density of excitations considered in the simulations

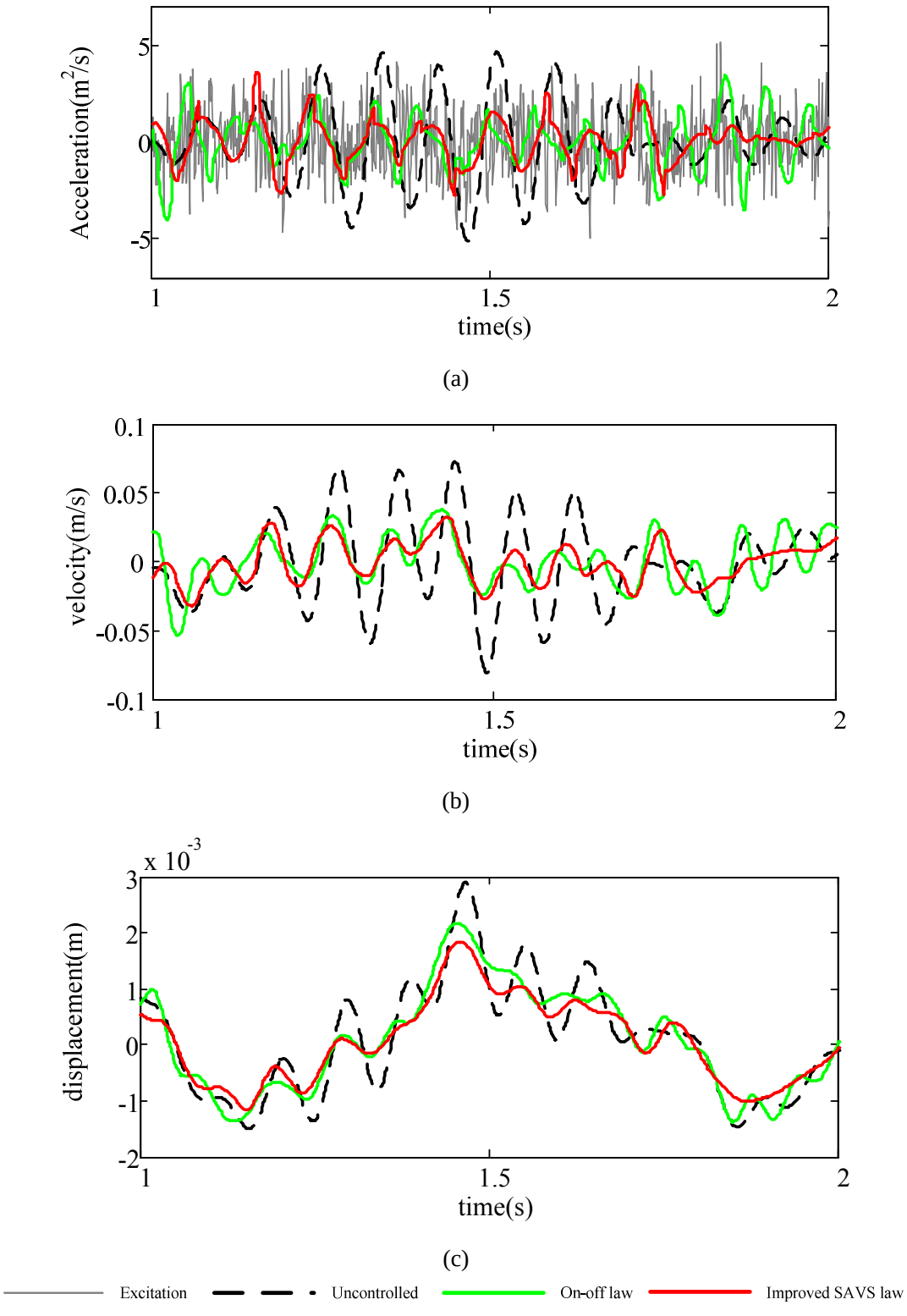

Figure 9 Responses of the SDOF system with different control laws

(a) Acceleration; (b) Velocity; (c) Displacement.

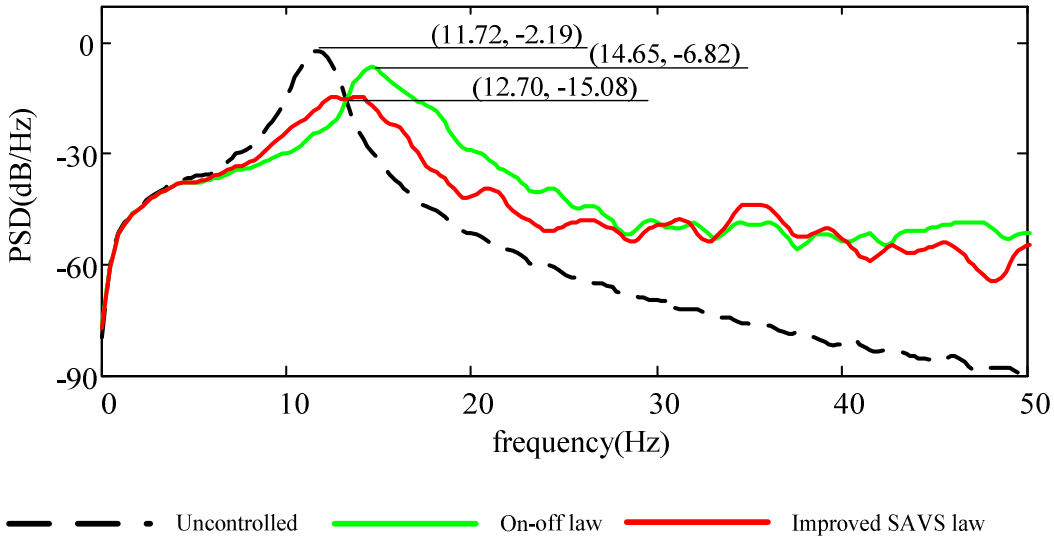

Figure 10 Power spectral density of the acceleration response of the SDOF system with different control laws

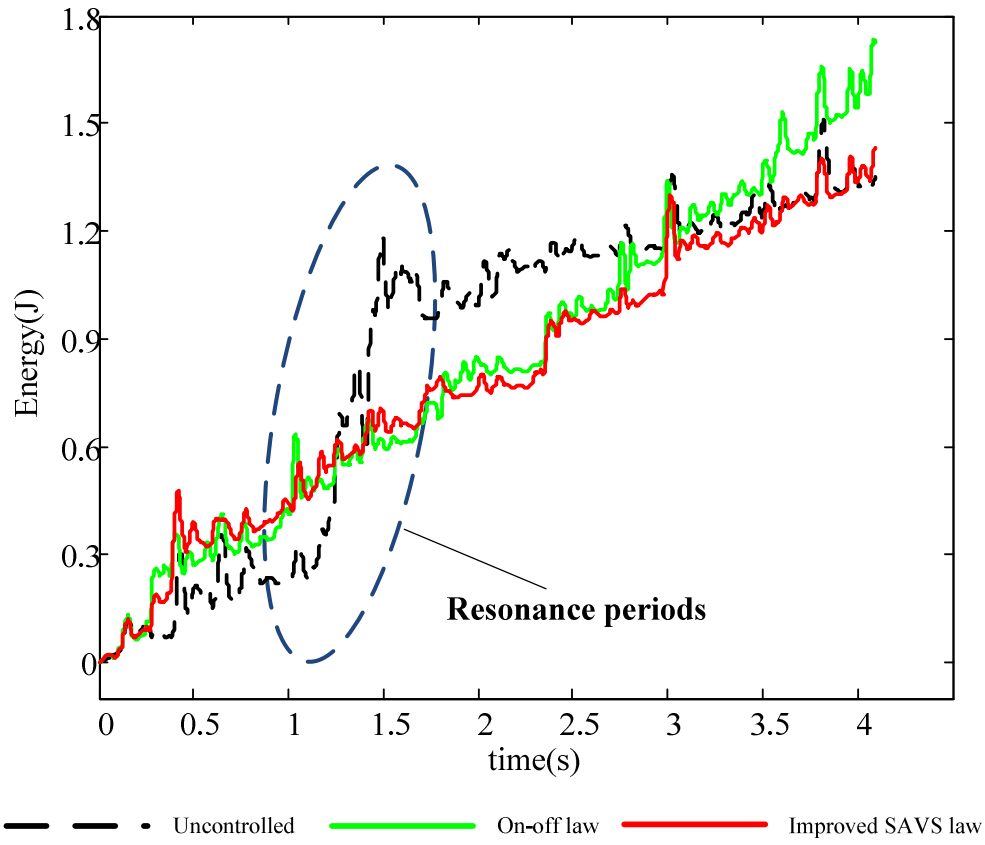

Figure 11 Total input energy of the SDOF system with different control laws

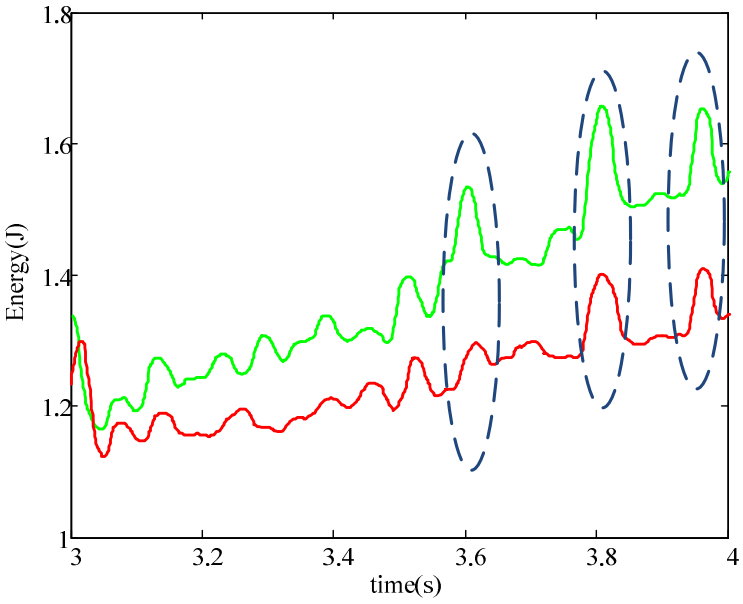

(a)

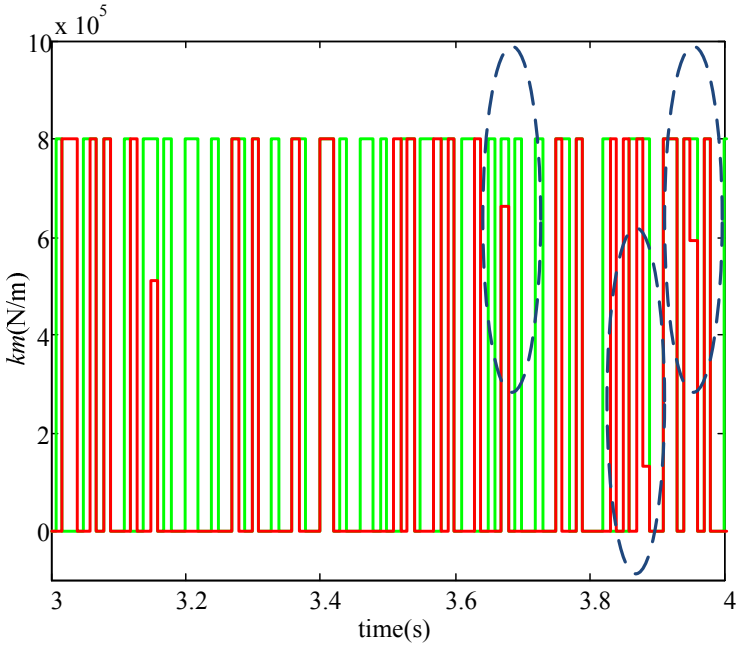

(b)

On-off law Improved SAVS law

Figure 12 Comparison of energy input and stiffness change

(a) E_{in} curves of the systems; (b) k_m of the system

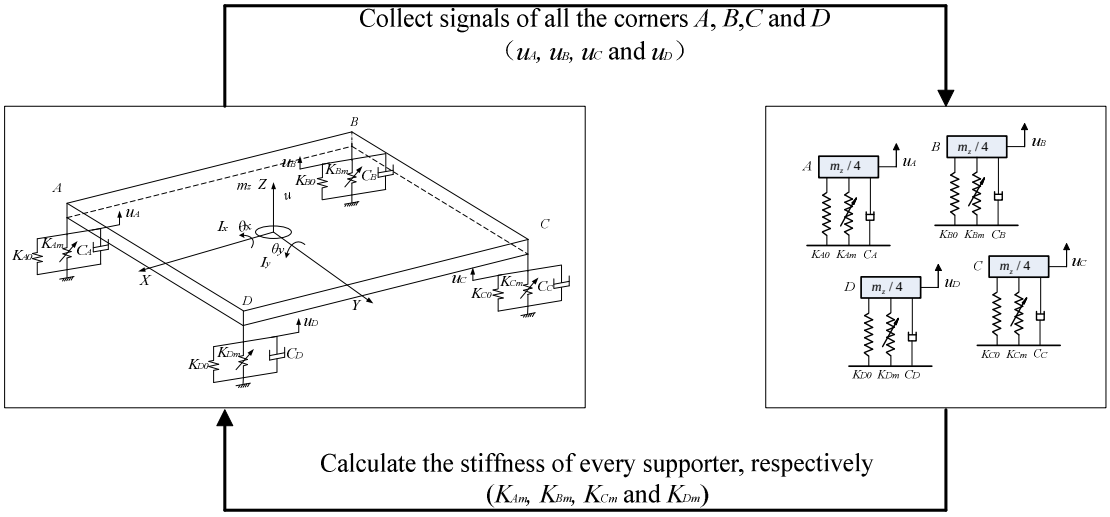

Figure 13 Schematic of control for an MDOF platform

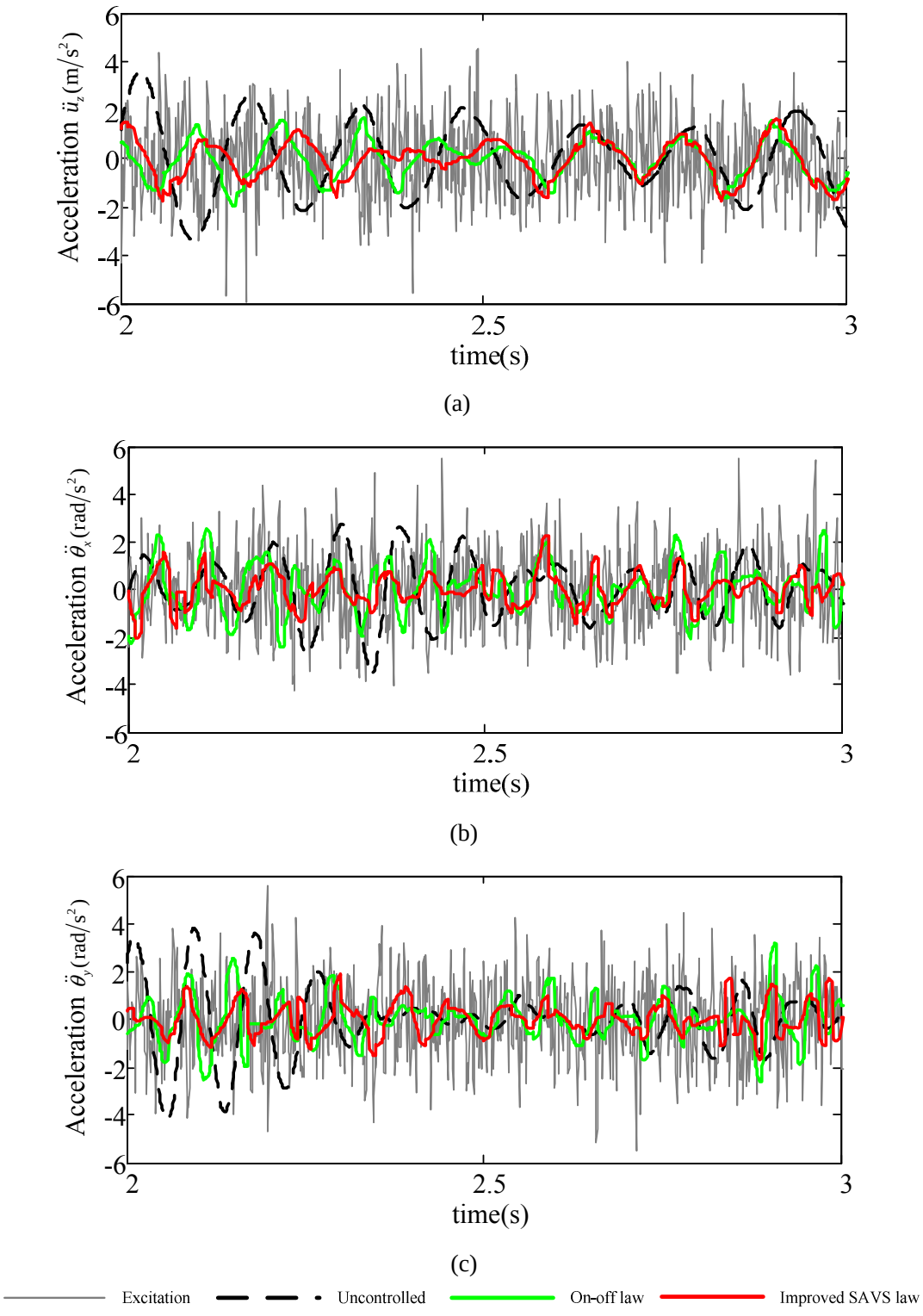

Figure 14 Acceleration time histories of the MDOF system with different control laws (a) $\ddot{u}_z$; (b) $\ddot{\theta}_x$; (c) $\ddot{\theta}_y$.

Table 1 η from different control laws for an SDOF system

η (%)	On-off law	Improved SAVS law
η_a	3	14
η_v	29	34
η_d	11	18

Table 2 η from different control laws for an MDOF system

η (%)	On-off law			Improved SAVS law		
	Z	X-rotation	Y-rotation	Z	X-rotation	Y-rotation
η_a	19	-2	-5	28	16	-2
η_v	44	34	16	45	42	20
η_d	20	5	2	19	6	5